Available online at www.sciencedirect.com

ScienceDirect

Procedia Structural Integrity 62 (2024) 781–788

Structural Integrity Procedia

www.elsevier.com/locate/procedia

II Fabre Conference – Existing bridges, viaducts and tunnels: research, innovation and applications (FABRE24)

Dynamic measurements and finite element analysis of a composite steel-concrete highway girder bridge

I. Vangelisti*, P. Di Re, J. Ciambella, A. Paolone

Department of Structural and Geotechnical Engineering, Sapienza University of Rome, Via Eudossiana 18, 00184, Italy

Abstract

This study focuses on the Operational Modal Analysis and numerical modeling of a steel-concrete girder bridge of the Italian highway network that has been subjected to extensive retrofit. A thorough experimental campaign is conducted, including in situ tests to measure the dynamic behavior of the bridge under wind or seismic loads. The test data are used to identify the modal parameters of the bridge and to calibrate a finite element model of the structure that reflects its current state. The finite element model is then adopted to perform sensitivity analyses for different scenarios of heavy vehicle traffic. The results help to understand how the bridge reacts to different loading conditions.

Keywords: finite element analysis; bridges health monitoring; structural dynamics; composite bridge.

1. Introduction

With the aging of highway and railway networks, understanding the structural behavior of existing bridges has become a paramount concern for public administrations and scientific communities. It is imperative to develop efficient control strategies that allow monitoring of degradation levels and prevention of critical conditions. In line with this objective, conducting in situ investigations and laboratory tests to characterize the static and dynamic response of bridges under possible critical actions has become an essential requirement, outlined in various technical

* *E-mail address:* vangelisti.2041240@studenti.uniroma1.it

10.1016/j.prostr.2024.09.106

codes. These investigations aim at creating a digital twin model of the structures by incorporating data collected from the tests, thus reflecting the current state of the bridges.

In this study, this approach is applied to a composite steel-concrete girder bridge of the Italian highway network. A comprehensive experimental campaign is conducted, involving in situ tests to characterize the dynamic response of the structure under potential wind or seismic excitations. The data acquired from these tests are used for the modal identification of the bridge and to calibrate a finite element model of the structure that is used to perform sensitivity analyses under the passage of heavy vehicles with varying path and transit speeds.

2. Description of the bridge structure

The bridge studied belongs to the Italian A24 "Roma-Teramo" highway. The structure has recently been subjected to extensive retrofit works that have modified its structural features.

The final configuration consists of two identical constructions, symmetric with respect to the longitudinal-vertical plane, each supporting one of the two separate carriageways of the highway. Figure 1 and figure 2 show the longitudinal and the transverse sections of the bridge, respectively. Each structure is made of an eight-spans composite steel-concrete girder deck, composed of two I-shaped continuous S355 steel beams, transversally connected by a series of I-shaped S355 steel cross girders, placed at a variable spacing, from 4 m to 6 m. The deck is realized with a 35 cm thick concrete C35/45 slab. The outer spans are 37 m long; the inner spans are 38 m long, for a total length of 302 m.

Bridge piers are constructed with a composite steel-concrete structure, which includes a circular C30/37 concrete core wrapped by a S355 Corten steel outer casing. The pier caps are trapezoidal-shaped steel elements. Besides, the abutments consist of a prismatic RC structure. Friction pendulum seismic isolators provide for the connection between the deck and substructure.

It is important to note that, during the construction process of the viaduct, the two structures defining the two carriageways are initially independent from each other. Subsequently (after almost one year), they are connected at the concrete slab level with a concrete curb that runs along the longitudinal centerline of the deck, as shown in figure 2. The effects of this connection are investigated in this work.

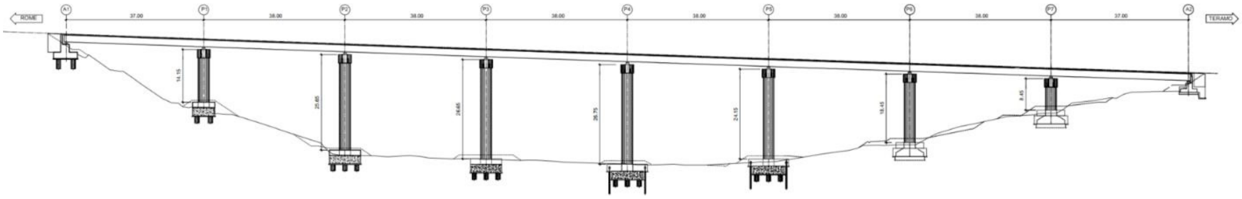

Fig. 1. Longitudinal profile of the bridge.

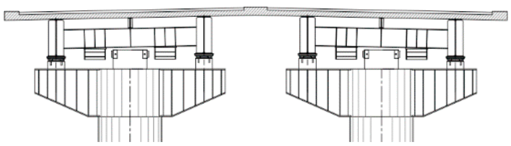

Fig. 2. Transverse section of the deck of the viaduct.

3. Finite element modeling and modal analysis

3.1. Finite element modeling of the bridge

The bridge finite element model is developed in SAP2000. The steel girder and the concrete slab are modeled with frame and shell elements, respectively. An appropriate mesh is used for these elements, based on a convergence analysis of the modal response performed for a single span model. The shells representing the concrete slab are connected in the vertical direction with the frames representing the steel beams using rigid links. The deck modeling is completed with the introduction of lateral concrete curbs as frame elements.

Piers and pier caps are also modeled as frame elements, and the abutments, given their limited influence on the dynamic response of the viaduct, are assumed as infinitely rigid and, thus, included in the model as nodal restraints.

The connection between the deck and the substructures is modeled by using rigid and elastic links: rigid links connect the pier cap to the base of the seismic isolators and the top of the isolators to the intrados of the longitudinal steel beams; two-node elastic springs, working on the three translational relative displacements along x, y and z directions, represent the seismic isolators.

Figure 3 shows a detail of the of isolator modeling (left) and the complete model of the bridge (right).

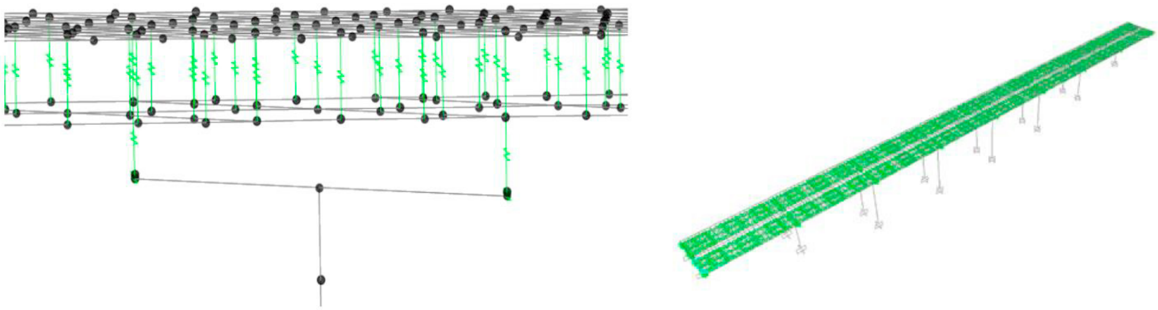

Fig. 3. Detail of seismic isolators modeling (left) and complete double roadways finite element model of the bridge (right).

3.2. Modal analysis of the single carriageway model

Modal analysis is first performed with a finite element model that represents only one of the two carriageways. The vibration modes obtained from this model can be classified into vibration modes that consider: rigid translations and rotations of the deck; flexural deformation of the deck in the horizontal plane x-y; torsional deformation of the deck involving the piers; flexural deformation of the piers; flexural deformation of the deck in the vertical plane x-z; and torsional deformation of the deck.

Figure 4 shows the first flexural and first torsional mode shapes, while table 1 shows the frequency values of seven significant modes.

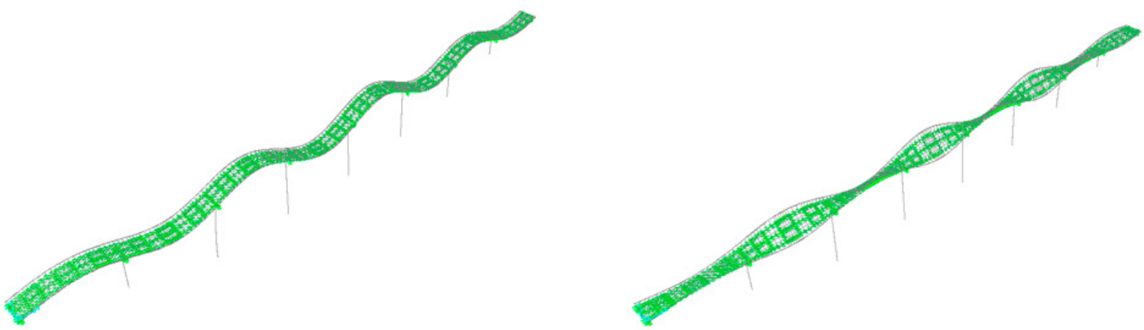

Fig. 4. First flexural mode shape (left) and first torsional mode shape (right).

To investigate the coupling between the deck and pier response, the same analysis is conducted by adopting a finite element model where, as limit case, the piers are assumed as infinitely rigid. The results of this analysis, not reported here for brevity, show similar values of the frequencies and similar deformed shapes for the modes involving the deck deformations. This indicates a high level of dynamic independence between the deck and the substructures.

Table 1. Frequency values of 7 significant modes of vibration of the bridge.

Mode number	Mode classification	Frequency [Hz]
1	Rigid Ux	0.34
2	Rigid Uy	0.35
3	Rigid Uz	0.36
4	Flexural x-y 1	0.58
6	Piers-deck torsional 1	1.98
11	Flexural 1	2.17
18	Torsional 1	2.97

3.3. Longitudinal curb modeling and modal analysis of the complete model

Sensitivity analysis is performed to identify the optimal approach for modeling the longitudinal curb that connects the two carriageways. Therefore, three alternative approaches are considered: the use of shell elements, the use of infinitely rigid frame elements, and the use of rigid links.

Modal frequencies and shapes involving the deck and resulting from the three analyses are compared with those obtained for the single carriageway model. With reference to the flexural modes of the deck, the differences among the approaches are extremely limited. However, frequencies tend to deviate from the previous values when considering the torsional modes, which involve deck and pier deformation, with a maximum of about 5% difference. This difference further increases for the modes that simultaneously involve both carriageways, up to 25% for pure torsional modes of the deck, and 45% for flexural modes in the deck plane. Despite the expected differences between single and double carriageway models, modal frequencies and shapes of other modes do not depend on the curb modeling approach (shells, rigid frames or rigid links), with less than 1% discrepancy among the investigated cases, showing that, for this structure, the three modeling approaches are equivalent. For the additional analyses reported in this work, shell elements are adopted, since these are more consistent with the shell modeling of the rest of the deck.

4. Operational Modal Analysis and model updating

The finite element model described above is developed referring to the geometric and material data gathered during a preliminary in situ survey. As usual, these data may be affected by important uncertainties that can be reduced by exploiting the information obtained from structural monitoring. A possible framework consists in conducting Operational Modal Analysis (OMA) to assess the bridge dynamic properties, such as modal frequencies, shapes, and damping ratios. Hence, the model is updated to reduce the difference between numerical and measured results.

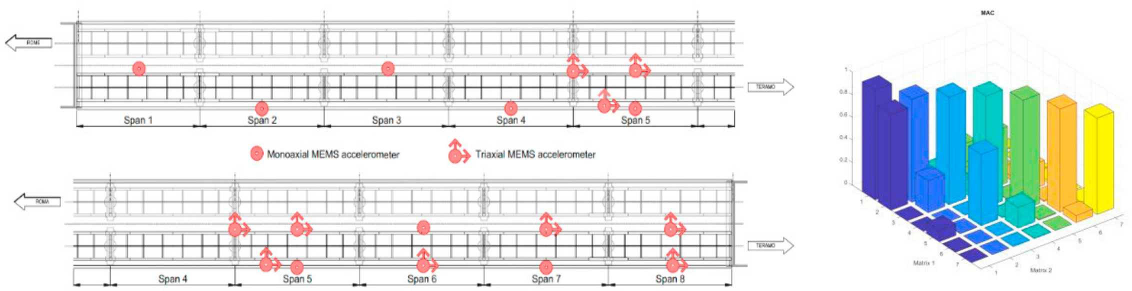

Fig. 5. Sensor layout on the right carriageway of the viaduct (left) and MAC between numerical and experimental mode shapes (right).

4.1. Operational Modal Analysis

The OMA is conducted on the right carriageway of the viaduct, recording, in a 30-minute time frame, the bridge dynamic response under environmental excitation and under the passage of a heavy vehicle over a speed bump. Measurements are obtained by means of a layout of monoaxial and triaxial MEMS accelerometers, as shown in figure 5. Modal frequencies of the bridge are extracted from the recorded data by performing a Frequency Domain Decomposition (FDD). The corresponding modal shapes are validated according to the Modal Assurance Criterion (MAC). Only those modes for which MAC > 0.85 (figure 5) are considered as effective vibration modes.

4.2. Model updating

The updating of the finite element model is performed by considering the stiffness of the materials. For each value of these parameters, the average difference between numerical and experimental frequencies of the previously identified modes is calculated, according to the following objective function:

$$e = \sqrt{\frac{1}{n}\sum_{i=1}^{n}\left(\frac{f_{i,num}-f_{i,exp}}{f_{i,exp}}\right)^2} \tag{1}$$

where n is the number of modes used for the updating process, $f_{i,num}$ is i-th numerical frequency and $f_{i,exp}$ is i-th experimental frequency. The stiffness of the concrete of the piers has a very limited influence on the total error, since the modes included in the optimization marginally involve the piers; thus, only the stiffness of the concrete of the deck, E_{deck}, and that of the steel, E_{steel}, are included in the evaluation, by operating first on E_{steel} and then on E_{deck}. The updated values for these parameters are listed in table 2 and compared with the initial ones. Once the model is updated, the bridge digital twin is obtained, and it can be used as a reference to develop studies and analyses of its structural behavior, as shown in Section 4.

Table 2. Stiffness parameter of the FEM model: initial and updated values.

Stiffness parameter	Initial value [MPa]	Updated value [MPa]	Difference [%]
E_{steel}	210	215.3	+2.5 %
E_{deck}	34.1	30	-10%

5. Dynamic response of the viaduct under different loading conditions

The updated model is used to perform sensitivity analyses to investigate the response of the structure when subjected to a forced vibration due to the passage of heavy vehicles, for varying paths and transit speeds. Vehicle features and load paths are defined according to the Italian provisions for construction NTC2018. Thus, a two-axle tandem vehicle with 300 kN for each axle is adopted, moving on the load paths numbered from 1 to 3, as indicated in figure 6.

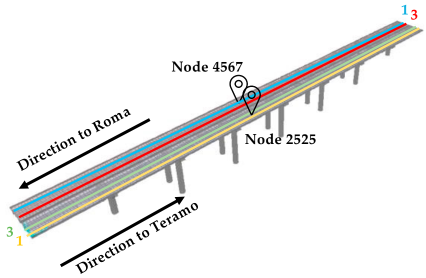

Fig. 6. Load path and investigated nodes for dynamic analyses.

Linear elastic time history dynamic analyses are performed under the moving vehicle load, based on modal decomposition, with the use of the first 300 modes. Modal decomposition-based time history analysis is chosen over direct integration method since it is computationally less onerous and sufficiently accurate. For the sake of simplicity, the single carriageway model is hereafter labeled as model A and the double carriageway model is labeled as model B.

For each model, time history of displacement and acceleration of the two nodes, no. 2525 and no. 4567, located at the fourth midspan of span, moving from Rome to Teramo, (figure 6) were computed, together with those of the total bending moment of the deck section located at the same midspan.

5.1. Dynamic response of single and double model for different transit speed

In a first scenario, analyses are carried out on model A, for a variable vehicle speed ranging from 30 to 130 km/h, with variation step of 20 km/h. The vehicle is moving on lane 1. Figure 7 presents displacement and acceleration time histories of node 2525 (loaded carriageway) and bending moment of the mid-span for 70 km/h speed transit.

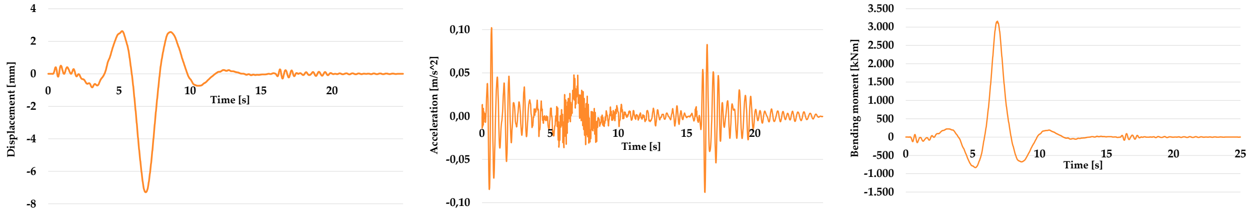

Fig. 7. Displacement (left), acceleration (center) and bending moment (right) time history for 70 km/h transit.

Displacement and bending moment peaks are recorded when the vehicle transits over the monitored node (figure 7 left). Three peaks are obtained for the acceleration: the first one corresponds to the beginning of the load transits, the second to the passage of the vehicle on the studied midspan, and the third to the beginning of the free vibration. The maximum of the three peaks is obtained when the load transit begins, due to the inertial perturbation that the vehicle generates on the bridge. Moreover, displacement and bending moment peaks are contemporary.

In a second scenario, model B is used. Load path and speed are the same as those of the first scenario. Figure 8 summarizes the displacement, acceleration and bending moment time histories for node 2525 and node 4567 and the corresponding mid-span sections.

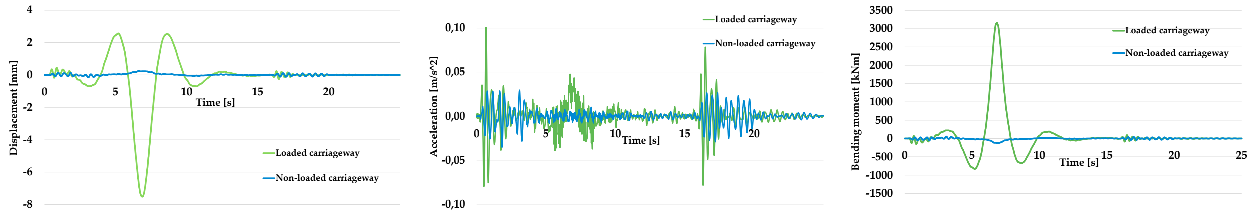

Fig. 8. Displacement (left), acceleration (center) and bending moment (right) time histories for scenario 2.

Displacement, acceleration, and bending moment trends of the loaded carriageway are very similar to those of the first scenario (model A). Conversely, the non-loaded carriageway shows a negligible response in terms of displacement and bending moment, while acceleration is comparable, although lower, to the one of the loaded carriageway. The limited response of the non-loaded carriageway in terms of displacement and bending moment suggests that model A considering only one carriageway provides accurate results and can correctly describe the response of the entire bridge, i.e., the coupling between the two carriageways is negligible.

Figure 9 shows the dynamic amplification factors for the displacement (left) and bending moment (right), calculated with reference to the static case. Two aspects are highlighted: maximum displacements of the loaded carriageway are not affected by dynamic amplification and, thus, are not influenced by the vehicle speed; dynamic amplification is more noticeable for the non-loaded carriageway, but this feature has limited influence, due to the low values of the absolute displacements obtained for this carriageway, as shown in figure 9. Furthermore, the figure shows a very similar prediction of the loaded carriageway response obtained from models A and B, confirming the possibility of using model A to characterize the behavior of the entire bridge, with significantly lower computational burden.

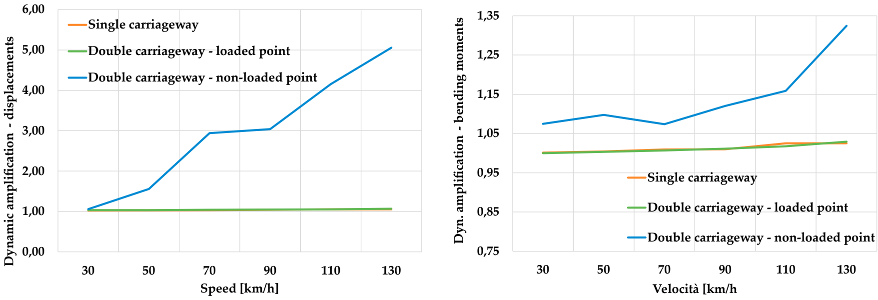

Fig. 9. Dynamic amplification of the displacement (left) and bending moment (right), for varying speed, in model A and B.

5.2. Dynamic response to varying load path

Two additional scenarios are finally examined to study the influence of the different the loading paths. Model B is considered. In the first scenario, the results of the vehicle transiting on lane 1 are compared with those of the vehicle transiting on lane 3, both at 70 km/h speed. Figure 10 shows the displacement time history for the loaded (left) and non-loaded (left) carriageways.

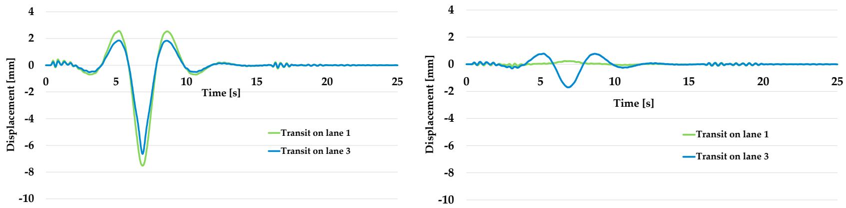

Fig. 10. Displacement time history for the loaded (left) and non-loaded (right) roadways for the the transit of the vehicle on lanes 1 and 3.

The maximum displacement of the loaded carriageway decreases, albeit slightly, as the vehicle travels on lane 3 instead of lane 1 (figure 10 left). This is an expected result that can be ascribed to a greater dynamic involvement of the non-loaded carriageway in the bridge response, consistently confirmed by the increase in its maximum displacement (figure 10 right, blue curve).

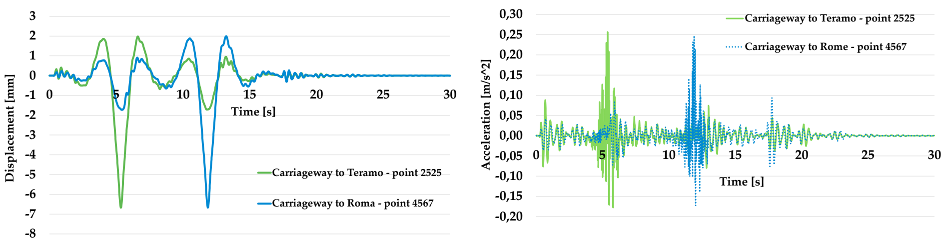

Fig. 11. Displacement (left) and acceleration (right) time histories for the contemporary transit of the vehicle on lane 3 to both directions.

In the second scenario, the contemporary transit of two vehicles at 90 km/h is analyzed. The first vehicle moves on lane 3 of the carriageway directed to Rome, while the second moves on lane 3 of the carriageway directed to Teramo. The passages of the two vehicles are temporally offset by 7 seconds. Results are shown in figure 11. Displacement and acceleration time histories show typical trends with two peaks. The maximum values are related to the transit of the vehicle on the point under investigation. The minor peaks are obtained when the vehicle transiting on the opposite carriageway passes in correspondence of the monitored point.

6. Conclusions

In this paper, the dynamic response of an eight-spans composite steel-concrete highway continuous beam viaduct was analyzed. A finite element frame-shell model of the structure was developed: the steel girder, the concrete curbs and the piers were modeled by using frame elements and the concrete slab was modeled by using shell elements. Alternative approaches for modeling the longitudinal curb, that connects the two carriageways running along the centerline of the deck, were investigated. Based on this analysis, shell elements were adopted, providing for a transversely rigid element.
A model updating procedure was performed by varying the stiffness of the materials to minimize the error between numerical and experimental frequencies, the latter extracted from the dynamic measurements gathered on the bridge. The updated model was used to perform modal decomposition-based time history analyses under the passage of heavy vehicles. Displacement, acceleration and bending moment time histories of two investigated cross-sections of the bridge were studied to explore the influence on the dynamic response of varying speeds and load paths, and to study the grade of coupling between the two carriageways.
The obtained results show a negligible coupling between the two carriageways, despite the presumed connection between them due to the presence of the transversely rigid longitudinal curb. This aspect is confirmed by evaluating the displacement time history of the non-loaded carriageway, which results extremely limited when the vehicle transits on the other carriageway, even if the load path varies from lane 1 to lane 3, approaching the non-loaded carriageway. Hence, according to the showed decoupling, a single carriageway model could correctly describe the response of the entire bridge, with a lower computational burden. Furthermore, the analysis highlighted a limited dynamic amplification of displacements and accelerations, confirming that the amplitude of the bridge response does not depend on the transit speed.

References

Peeters, B., De Roeck, G.: One-year monitoring of the Z24-Bridge: environmental effects versus damage events, Earthquake Engineering & Structural Dynamics, 30 (2), 149-171 (2001).

Di Re, P., Lofrano, E., Ciambella, J., Romeo, F.: Structural analysis and health monitoring of twentieth-century cultural heritage: The Flaminio Stadium in Rome, Smart Structures and Systems, 27 (2), 285-303 (2021)

Chung, W., Sotelino, E.D.: Three-dimensional finite element modeling of composite girder bridges, Engineering Structures, 28 (1), 63-71 (2006).

Kaliyaperumal, G., Imam, B., Righiniotis, T. : Advanced dynamic element analysis of a skew steel railway bridge, Engineering Structures, 33, 181-190 (2011).

Pastora, M., Binda, M., Harcarik, T.: Modal Assurance Criterion, Procedia Engineering, 48, 543-548 (2012).

Di Re, P., Ciambella, J., Lofrano, E., Paolone, A.: Dynamic test and modeling span interaction in high-speed railway girder bridges, measurement, *under review*.

Peeters, B., De Roeck, G., One‐year monitoring of the Z24‐Bridge: environmental effects versus damage events. Earthquake engineering & structural dynamics, 30(2), 149-171, 2001.

Qu, C.X., Yi, T.H., Li, H.N., Chen, B., Closely spaced modes identification through modified frequency domain decomposition. Measurement: Journal of the International Measurement Confederation, 128(May), 388-392, 2018.

Liu, K., Lombaert, G., De Roeck, G., Dynamic analysis of multispan viaducts with weak coupling between adjacent spans. Journal of Bridge Engineering, 19(1), 83-90, 2014.

Xu, H., Li, W.L., Dynamic behavior of multi-span bridges under moving loads with focusing on the effect of the coupling conditions between spans. Journal of Sound and Vibration, 312(4-5), 736-753, 2008.

Chung, W., Sotelino, E.D., Three-dimensional finite element modeling of composite girder bridges. Engineering Structures, 28(1), 63-71, 2006.

Zhu, X.Q., Law, S.S., Moving load identification on multi-span continuous bridges with elastic bearings. Mechanical Systems and Signal Processing, 20(7), 1759-1782, 2006.